Carcinogenesis vol.32 no.3 pp.262–270, 2011
doi:10.1093/carcin/bgq249
Advance Access publication November 19, 2010

L1-CAM expression in ccRCC correlates with shorter patients survival times and confers chemoresistance in renal cell carcinoma cells

Kai Doberstein, Anja Wieland[1], Sophia B. Boyoung Lee, Roman A. Alexander Blaheta[2], Steffen Wedel[2], Holger Moch[3], Peter Schraml[3], Josef Pfeilschifter, Glen Kristiansen[3] and Paul Gutwein*

Pharmacology, pharmazentrum frankfurt/ZAFES, University Hospital Goethe University Frankfurt, D 60590 Frankfurt am Main, Germany, [1]Institute of Reconstructive Neurobiology, Life & Brain Center, University of Bonn and Hertie Foundation, D 53127 Bonn, Germany, [2]Department of Urology and Pediatric Urology, Goethe University Frankfurt, D 60590 Frankfurt am Main, Germany and [3]Institute of Surgical Pathology, University Hospital Zurich, University of Zurich, 8091 Zurich, Switzerland

*To whom correspondence should be addressed. pharmazentrum frankfurt, Klinikum der Johann Wolfgang Goethe-Universität Frankfurt, Theodor-Stern-Kai 7, D-60590 Frankfurt am Main, Germany. Tel: +49 69 6301 4920; Fax: +49 69 6301 79 42;
Email: p.gutwein@med.uni-frankfurt.de

Conflicting data exist about the expression of L1 cell adhesion molecule (L1-CAM) in clear cell renal cell carcinoma (ccRCC). To determine the clinical usefulness of L1-CAM as a therapeutic or prognostic marker molecule in renal cancer patients, we analyzed its expression on a cohort of 282 renal cell carcinoma (RCC) patients. L1-CAM expression was found in 49.5% of 282 renal cancer tissues. Importantly, L1-CAM expression in patients with ccRCC was associated with significantly shorter patient survival time. We further present evidence that L1-CAM was involved in the resistance against therapeutic reagents like rapamycin, sunitinib and cisplatin. The downregulation of L1-CAM expression decreased renal cancer cell proliferation and reduced the expression of cyclin D1. In addition, we found out that Von Hippel-Lindau (VHL) deficiency was accompanied by a downregulation of the transcription factor PAX8 and L1-CAM. In normal renal tissue, PAX8 and L1-CAM were co-expressed in collecting duct cells. Importantly, the downregulation of PAX8 by small interfering RNA increased the expression of L1-CAM and concomitantly induced the migration of renal cancer cells. Furthermore, we observed in 65.3% of 282 RCC patients a downregulation of PAX8 expression. With chromatin immunoprecipitation analysis, we additionally demonstrate that PAX8 can bind to the promoter of L1-CAM and we further observed that the downregulation of PAX8 was accompanied by increased L1-CAM expression in a high fraction of ccRCC patients. In summary, we show that VHL and PAX8 are involved in the regulation of L1-CAM in renal cancer and L1-CAM represents an important therapeutic and prognostic marker protein for the treatment of ccRCC.

Introduction

Renal cell carcinoma (RCC) accounts for 2–3% of all malignant diseases in adults (1). The incidence of RCC is rising worldwide and is ~209 000 cases/year and 102 000 deaths/year (2). Although the 5 years survival is 60% overall for kidney cancer, it drops to 10% in patients with metastatic disease (3). Therefore, alternative approaches are urgently required to prolong patient survival since very few effective therapeutic regimens are available. In this context, L1 cell adhesion molecule (L1-CAM) has been shown to be an interesting target protein for the treatment of different types of cancer (4). L1-CAM belongs to the immunoglobulin superfamily of cell adhesion molecules and it consists of six immunoglobulin-like domains, five fibronectin type 3 repeats, a single transmembrane region and a short cytoplasmic tail (5). In addition to the transmembrane form of L1-CAM, a soluble form of L1-CAM can be released from the cell surface or in released vesicles through the activity of ADAM10 (6).

So far, the data on L1-CAM expression in clear cell renal cell carcinoma (ccRCC) are contradictory. Allory *et al.* (7) has reported that 47% of ccRCC analyzed were positive for L1-CAM, whereas Huszar *et al.* (8) showed that ccRCC did not express L1-CAM. Intriguingly, it has been reported that L1-CAM expression in ccRCC correlated with metastasis (7). L1-CAM is often not expressed in normal tissue, but induced expression can be found in melanoma, ovarian and breast cancer (9). The presence of L1-CAM in cancer tissue is commonly correlated with a poor prognosis and more advanced stages of the disease; therefore, it is of great importance to identify factors, which regulate L1-CAM in cancer cells. In the nervous system, it has been shown that the transcription factor PAX6 is able to activate L1-CAM expression (10). In the kidney, PAX2 and PAX8 are the best-characterized family members and it is known that both factors play crucial roles in the developing kidney by specifying the nephric lineage (11). In addition to fetal tissue, PAX2 overexpression has been found in several human tumors like ovarian, breast and ccRCC (12). Recently, hypoxia and the loss of Von Hippel-Lindau (VHL) function has been linked to PAX2 upregulation (13). The best-described function of VHL as a transcriptional regulator is its ability of targeting the α subunits of hypoxia inducible factor for ubiquitin-mediated proteolysis. It is well-known that the loss of VHL in ccRCC, which is a common event, provokes cell invasion, angiogenesis and tumor cell survival (14). In this study, we analyzed the expression of L1-CAM and PAX8 in 282 clinically characterized RCC cases and correlated their expression with patient's survival. We provide evidence that VHL is involved in the regulation of L1-CAM in RCC. Furthermore, knockdown of L1-CAM abrogated the chemoresistance of renal cancer cells against cisplatin, which endorses that targeting L1-CAM represents a promising therapeutic option in the treatment of ccRCC.

Abbreviations: ChIP, chromatin immunoprecipitation; ccRCC, clear cell renal cell carcinoma; L1-CAM, L1 cell adhesion molecule; mRNA, messenger RNA; PCR, polymerase chain reaction; RCC, renal cell carcinoma; siRNA, small interfering; TMA, tissue microarray; VHL, Von Hippel-Lindau; WT, wild-type.

Materials and methods

Antibodies

The VHL antibody was ordered from Santa Cruz Biotechnology, Heidelberg, Germany. The monoclonal antibodies L1 11A and L1 14.10 were a kind gift from Prof. Peter Altevogt (German Cancer Center, Heidelberg, Germany). The polyclonal PAX8 antibody was a kind gift from Prof. Roberto Di Lauro (Stazione Zoologica Anton Dohrn, Napoli, Italy). For western blot analysis, the Hemagglutinin tag antibody (Abcam plc, Cambridge, UK), Histone deacetylase antibody (Santa Cruz Biotechnology, Santa Cruz, CA) and β-actin antibody (Sigma–Aldrich, St Louis, MO) were used.

Cell culture

The renal carcinoma cell lines A-498 and 786-O were obtained from Prof. Wilhelm Krek (Institute of Cell Biology Zürich, Switzerland) and are described elsewhere (15). The renal cancer cell line Föhn was a kind gift from Prof. Altevogt (German Cancer Research Center, Heidelberg, Germany). Cells were grown under normoxic (21% O_2) or hypoxic (1% O_2) in a Napco 7001 incubator (Precision Scientific, Chennai, India).

Membrane isolation, protein extraction and western blot analysis

Membrane fractions were isolated by incubating the cells for 10 min in hypolysis buffer [10 mM Tris–HCl pH 8.0, 0.1 mM dithiothreitol, Protease Inhibitor complete (Roche Diagnostic, Penzberg, Germany)] at 4°C. Cell suspension was homogenized in a glass homogenizer and membrane proteins were centrifuged at 1000*g* at 4°C followed by a high-speed centrifugation at 100 000*g*. Protein lysates of renal cancer cells and western blot analysis were performed as described in ref. 16.

Nucleus isolation

Cells (1×10^7 cells) grown on a 10 cm dish were trypsinized and washed twice with phosphate-buffered saline and nuclear proteins were isolated as described in ref. 16.

Fluorescence microscopy

Cells were grown on coverslips and fixed with 4% paraformaldehyde/phosphate-buffered saline. Immunofluorescence stainings of cells or renal tissue sections were performed as described in ref. 17.

Complementary DNA synthesis and polymerase chain reaction analysis

RNA from cultured cells was isolated using the RNA Easy Kit according to the manufacturer's protocol (Qiagen, Hilden, Germany). Equal amounts of total cellular RNA (1 μg) were reverse transcribed with random primer by the use of M-MuLV Reverse Transcriptase (Fermentas, St Leon-Rot, Germany). Transcribed complementary DNAs were used for polymerase chain reaction (PCR) with specific primers for human L1-CAM (5′-GACTACGAGATCCACTTGTTTAAGGA-3′ and 5′-CTCACAAAGCCGATGAACCA-3′), PAX8 (5′-TCAACCTCCCTATGGACAGC-3′ and 5′-GCCTCGCTGTAGGAGGAGTATGTT-3′), PAX2 (5′-CCCAGCGTCTCTTCCATCA-3′ and 5′-CCACACCACTCTGGGAATCT-3′) and β-actin (5′-GGACTTCGAGCAAGAGATGG-3′ and 5′-AGCACTGTGTTGGCGTACAG-3′). PCR products were amplified using *Taq* DNA polymerase (NatuTec, Frankfurt, Germany) and subjected to electrophoresis through 2% agarose gels and ethidium bromide staining.

Real-time PCR

Real-time PCR was performed as described in the protocol from the Absolute Blue QPCR SYBR Green Low ROX Kit (Thermo Scientific, Hilden, Germany). The same primers that were used for the PCR were also used for the real-time PCR. The *C*(T) values of L1-CAM and PAX8 messenger RNA (mRNA) level were normalized to the *C*(T) values of β-actin mRNA within the same sample.

si RNA transfection

Small interfering RNA (siRNA) duplexes were used for the downregulation of PAX8 expression (PAX8-siRNA: 5′-UCUUUAUUUAUUACAUGAA-3′) and L1-CAM expression (L1-CAM-siRNA 5′-AGGGAUGGUGUCCACUUCAAATT-3′). As a negative control, unspecific scrambled siRNA duplexes (5′-AGGUAGUGUAAUCGCCUUGTT-3′) were applied. Twenty-four hours before transfection, 0.5×10^5 cells were seeded in six-well plates. Transfection of siRNA was carried out using Oligofectamine (Invitrogen, Karlsruhe, Germany) and 10 nM siRNA duplex per well as described in ref. 18.

Tissue microarray construction

We constructed a tissue microarray (TMA) from RCC diagnosed at the Institute of Surgical Pathology, Universitätsspital Zurich, between 1993 and 2003, as recently described (19,20). Two hundred and eighty-two renal carcinomas were represented on the TMA. Staging met the Union for International Cancer Control 2002 criteria. Histological classification and grading was performed according to the World Health Organization. The median patient age was 63 years (range: 29–88 years). Of 184 patients were men, 98 women. The majority of the carcinomas were of clear cell type ($n = 230$; 81.6%). The remaining RCC were of papillary ($n = 42$; 14.9%) and chromophobe ($n = 10$; 3.6%) types. The tumor-status (pT) for these cases was as follows: pT1—121 (42.9%), pT2—36 (12.8%) and pT3—125 (44.3%).

The Fuhrman grades were G1 in 3 (1.1%), G2 in 94 (33.3%), G3 in 120 (42.6%) and G4 in 65 (23.0%) cases, respectively. Disease-specific death occurred in 106 patients (37.6%) after a median survival time of 18 months (range 0–123). Data on the Eastern Cooperative Oncology Group performance status were not available. In the TMA, each tumor was represented by one tissue core (0.6 mm).

ccRCC test TMA

A test TMA consisting of seven ccRCCs with wild-type (WT) *VHL* and eight with frameshift mutations in *VHL* was generated as described in ref. 13.

TMA immunohistochemistry

The TMA blocks were freshly cut (3 μm) and mounted on superfrost slides (Menzel Gläser, Braunschweig, Germany). Immunohistochemistry was conducted with the Ventana Benchmark automated staining system (Ventana Medical System, Tucson, AZ) using Ventana reagents for the entire procedure. The L1-CAM and PAX8 antibodies were used at a concentration of 1:100. For detection, we used UltraVIEW™ DAB detection kit using the benchmarks CC1m-heat induced epitope retrieval. Slides were counterstained with hematoxylin, dehydrated and mounted.

Evaluation of TMA immunohistochemistry

The immunohistochemistry was evaluated by a single GU pathologist (G.K.) to minimize intraobserver variability. Intensity of immunoreactivity was semi-quantively scored as negative, weakly, moderately or strongly positive. A panel of representative figures was compiled before the systematic evaluation of the tumor cohort was used as a reference, which layed next to the microscope for continuous comparison.

Statistical analysis of immunohistochemistry data

The data were compiled with the software package SPSS, version 15.0 (SPSS Software, München, Germany). Spearman's Rho was used to assess the statistical significance of the correlation between molecular and clinicopathological parameters. Univariate survival analysis was performed according to Kaplan–Meier, and differences in survival curves were assessed with the log rank test. Additionally, univariate Cox models were calculated. Multivariate survival analysis was performed on all the parameters that were found to be significant on univariate analysis using the Cox regression model. $P < 0.05$ was considered statistically significant.

Nucleofection

Cells were nucleofected using materials supplied in the Amaxa Cell Line Optimization Nucleofector Kit™ (Lonza, Cologne, Germany). Föhn cells (2×10^6) were suspended in Cell Line Nucleofector Solution V (added with supplement) and mixed with 5 μg PAX8–pcDNA 3.1 plasmid DNA (kind gift of Prof. Vassart, Brussels, Belgium). Control cells were transfected with empty pcDNA 3.1 plasmid DNA. The nucleofected cells were transferred to a six-well plates containing fresh, prewarmed RPMI with 10% fetal bovine serum (0.7×10^6 cells per well) and maintained at 37°C.

Cell cycle analysis

Cells were seeded in six-well plates and transfected with siRNA as described before. Forty-eight hours after siRNA transfection, cells were left untreated or treated with 40 μM cisplatin (CDDP) for 24 h. Afterward, the cells were trypsinized, washed in phosphate-buffered saline and cell cycles analysis was performed as described in ref. 16. Data are presented by means ± standard deviations. Statistical and significant differences were determined using the Student's *t*-test.

Chromatin immunoprecipitation assay

The chromatin immunoprecipitation (ChIP)-IT Express kit (Active Motif, Rixensart, Belgium) was used to perform the ChIP assay. Four dishes (10 cm) of A498 renal cancer cells with 1×10^6 cells per dish were treated with 1% formaldehyde, followed by glycine stop solution. Afterward, cells were harvested, centrifuged and resuspended in lysis buffer. After 30 min of lysis and homogenization in a douncer, nuclei were collected and resuspended in shearing buffer. Enzymatic shearing was performed for 10 min to digest DNA in DNA fragments ranging in size from 200 to 500 bp. Afterward, 10 μl of the sheared chromatin was used as input control. The immunoprecipitation was performed overnight at 4°C using a head to head rotator. The incubation mixture containing 50 μl sheared chromatin, protein G magnetic beads and 3 μg PAX8 antibody (Proteintech Europe, Manchester, UK). After washing and elution, the samples were reverse cross-linked and treated with ribonuclease A and proteinase K. The DNA and the sheared chromatin input was directly used for PCR analysis. The primer pair 5′-GCAGCCAGCTCGCCGGCTCC-3′ and 5′-CAGCCCTGCACAGGATCGAG-3′ was designed to amplify a 129 bp product of the human L1-CAM promoter (GenBank-accession U52112).

Cell migration assay

Cell migration was measured as described (21). Each experiment was performed in triplicates and repeated at least three times. Data are presented by means ± standard deviations. Statistical and significant differences were determined using the Student's *t*-test.

Results

L1-CAM expression in ccRCC tissue correlates with shorter patients survival

Contradictory data exist about the expression of L1-CAM in ccRCC (7,8). Therefore, we analyzed the expression of L1-CAM by immunohistochemistry on a TMA with 282 renal tumor samples. For the immunohistochemistry analysis, we used a monoclonal antibody against L1-CAM (L1 14.10), which was also used in the study of Huszar *et al.* (8). Representative stainings of L1-CAM expression in normal kidney and tumor samples (negative, weak and strong expression) are shown in Figure 1A. The obtained results are summarized in a diagram (Figure 1B). Interestingly, from 282 stained renal tumors, 49.5% expressed L1-CAM. To further investigate the clinical usefulness of L1-CAM expression in RCC

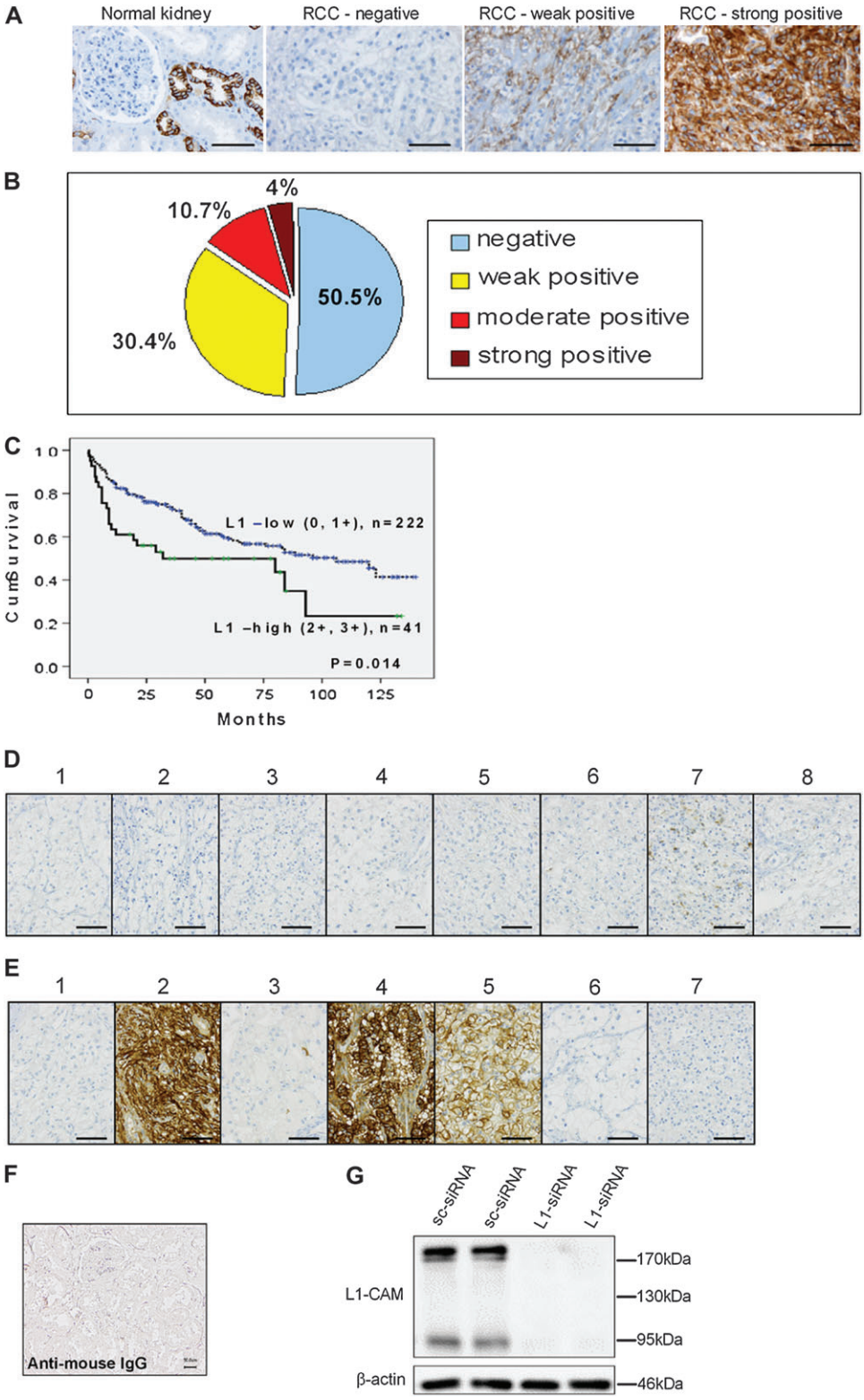

Fig. 1. Expression of L1-CAM in normal kidney and renal cancer on a TMA. (**A**) Immunohistochemistry images showing the expression of L1-CAM in normal kidney and a representative image of negative, weak positive and strong positive L1-CAM staining in renal cancer patients (RCC). Scale bars represent 50 μm. (**B**) Pie charts demonstrate the relative proportion of negative (blue), weak positive (yellow), moderate positive (red) and strong (maroon) L1-CAM-positive cases of RCC. (**C**) Kaplan–Meier survival analysis of the relationship between the expression of L1-CAM and the length of patient survival. Dotted line indicate patients with low levels of L1-CAM expression (n = 222), bold line represents patients with high levels of L1-CAM (n = 41). (**D**) L1-CAM expression in a TMA of eight ccRCC patients (1–8) with mutated VHL status. Scale bars represent 50 μm. (**E**) Immunohistochemical analysis revealed that three of seven patients with VHL WT ccRCC showed strong L1-CAM expression. Scale bars represent 50 μm. (**F**) Immunohistochemical staining with isotype-specific antibodies (anti-mouse igG) on human kidney sections was performed to determine the specificity of the monoclonal L1-CAM antibody (L1.14.10). (**G**) Seventy-two hours after the transfection of L1-CAM-specific siRNA, lysates of A498 VHL cells were prepared and western blot analysis with a monoclonal antibody against L1-CAM (L1 14.10) was performed. β-Actin was used to confirm equal protein loading.

patients, we compared the L1-CAM expression with the survival times of the analyzed patients. Postoperative follow-up data (median 40 months, range 1–140 months) were available for 264 patients. Importantly, L1-CAM expression in RCC tissue correlated with shorter patient survival times (Figure 1C, L1-CAM: relative risk = 1.8, $P = 0.014$). It is known that the majority of sporadic ccRCC is characterized by VHL gene mutations, which leads to a dysregulation of the function of the VHL protein (22). To analyze if VHL mutations are involved in the upregulation of L1-CAM in ccRCC, we investigated the expression of L1-CAM in a small TMA consisting of 15 ccRCC (eight with WT VHL and seven with VHL frameshift mutations). Surprisingly, six of seven VHL-mutated ccRCC did not express L1-CAM (Figure 1D), whereas in three of seven VHL WT ccRCC, a strong L1-CAM expression was detectable (Figure 1E). To confirm the specificity of the L1-CAM antibody (L1-14.10), we used an IgG isotype-specific antibody for our immunohistochemical staining on human kidney tissue (Figure 1F) and transfected L1-CAM-specific siRNA in A498 VHL cells to perform L1-CAM (antibody L1-14.10)-specific western blot analysis (Figure 1G).

L1-CAM expression is downregulated in VHL-deficient renal cancer cells

To investigate if the VHL protein is involved in the regulation of L1-CAM, we analyzed the L1-CAM expression in two VHL negative cell lines (A498 neo, 786-0 neo) and their WT VHL-expressing counterparts (A498 VHL and 786-0 VHL). Interestingly, we found in VHL-deficient cells significantly lower levels of L1-CAM protein compared with their WT counterparts (Figure 2A). With immunofluorescence analysis (Figure 2B) and western blot analysis of

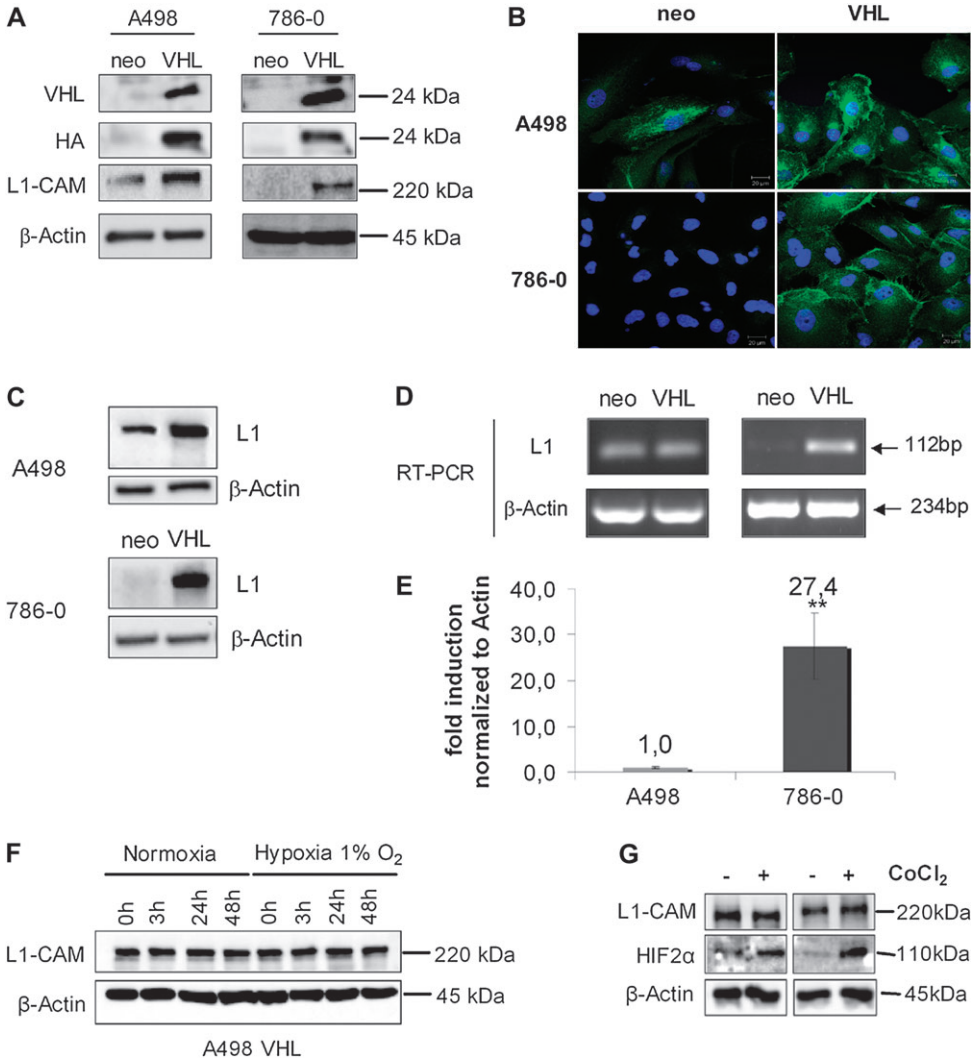

Fig. 2. L1-CAM expression is downregulated in VHL-deficient renal cancer cells. (**A**) Western blot analysis with VHL, Hemagglutinin antibody or L1-CAM-specific antibodies in lysates of A498 and 786 cells stable transfected with empty (neo) or Hemagglutinin-tagged VHL vector. Equal loading of protein samples were determined with β-actin-specific antibodies. (**B**) Immunofluorescence analysis of L1-CAM expression in A498 and 786-0 cells. A498 and 786-0 were incubated with an L1-CAM-specific antibody followed Alexa 488-coupled (green) secondary antibody. Scale bars represent 50 μm. (**C**) Membrane fractions from A498 and 786-0 cells were analyzed by western blot with L1-CAM-specific antibody. β-Actin was used to show equal protein loading. (**D**) mRNA was isolated from A498 and 786-0 cells and reverse transcription–PCR was performed with L1-CAM-specific primers. β-Actin was used as an internal control. (**E**) Real-time PCR results with L1-CAM-specific primers are depicted in a graph. The 786-0 VHL cells showed a 27.4-fold induction of L1-CAM mRNA compared with 786-0 neo cells. $^{*}P < 0.01$ considered statistically significant compared with 786-0 neo cells. (**F**) A498 VHL cells were treated for 3, 24 and 48 h under normoxic or hypoxic (1% O_2) conditions. Cell lysates were analyzed by L1-CAM-specific western blot. β-Actin was used to show equal protein loading. (**G**) A498 VHL cells were left untreated or treated for 24 h with 200 μM cobalt chloride ($CoCl_2$) and lysates were prepared and investigated by western blot analysis using L1-CAM or hypoxia inducible factor (HIF)-2α specific antibodies. β-Actin was used to determine equal protein loading.

isolated cell membranes (Figure 2C), we were able to confirm this data. Next, we isolated mRNA from the renal carcinoma cells and performed reverse transcription–PCR experiments. As shown in Figure 2D, only 786-0 VHL cells demonstrated higher levels of L1-CAM mRNA compared with its VHL-deficient counterpart. In contrast to 786-0 cells, L1-CAM mRNA levels in A498 neo and A498 VHL cells were not different (Figure 2D). These results were confirmed by real-time PCR (Figure 2E). To investigate if L1-CAM downregulation in VHL mutant renal cancer cells is hypoxia inducible factor dependent, we incubated the cells under hypoxic conditions. Importantly, hypoxia did not lead to a significant downregulation of L1-CAM protein expression in A498 VHL cells (Figure 2F). Similar results were obtained in 786-0 VHL cells (data not shown) and were confirmed by the treatment with the hypoxia mimicking reagent cobalt chloride (Figure 2G).

L1-CAM expression is involved in the chemoresistance of renal cancer cells against cisplatin

To determine the role of L1-CAM in renal cancer cell survival, we treated renal cancer cells with the chemotherapeutic agent cisplatin in the presence or absence of L1-CAM-specific siRNA. Interestingly, the knockdown of L1-CAM in 786-0 VHL cells alone increased the number of apoptotic cells (Figure 3A). Although 90% of the 786-0 VHL cells were resistant against 10 μg cisplatin treatment, the knockdown of L1-CAM led to a strong induction of apoptosis (7-fold) after 10 μg cisplatin treatment. In contrast to 786-0 VHL cells, the knockdown of L1-CAM alone did not induce apoptosis in A498 VHL (Figure 3B) and Föhn cells (Figure 3C), but both cell lines exhibited a significant induction of apoptosis after the treatment with 10 μg cisplatin (Figure 3B and C). The successful downregulation of L1-CAM by siRNA is depicted in each graph of Figure 3. In addition, we investigated if

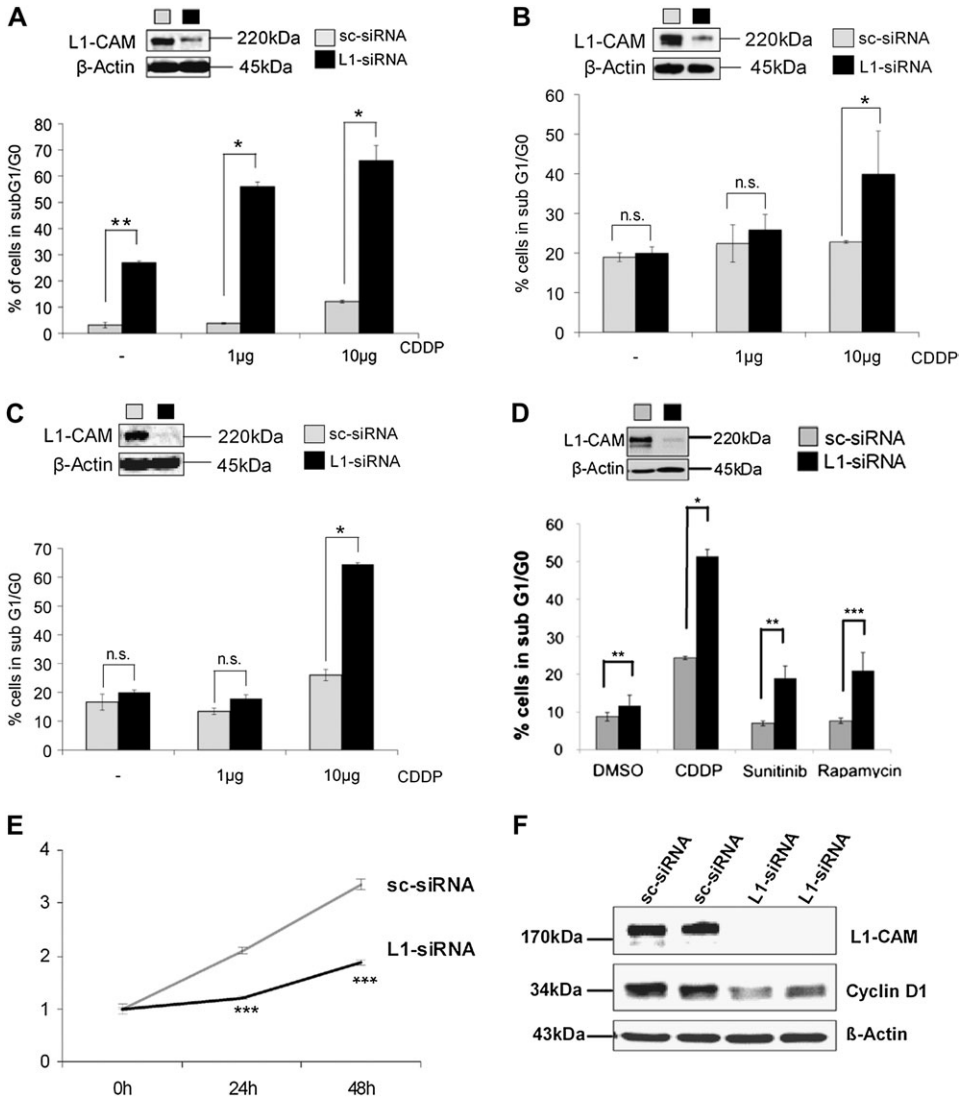

Fig. 3. Knockdown of L1-CAM in renal cancer cells increases cell death after cisplatin treatment (CDDP). 786-0 VHL (**A**), A498 VHL (**B**), Föhn cells (**C**) or A498 VHL cells (**D**) were transfected with scrambled (sc-siRNA) or L1-CAM-specfic siRNA (L1-siRNA). Forty-eight hours after transfection, cells were left untreated (−) or treated for 24 h with 1 or 10 μg cisplatin (CDDP), sunitinib (5 μM) or rapamycin (20 ng/ml) and cell cycle analysis were performed. Graph represents the percentage of cells in subG$_1$/G$_0$ phase (apoptotic cells), after the treatment with CDDP. $^{*}P < 0.05$ considered statistically significant compared with sc-siRNA-transfected cells treated with cisplatin (sc-siRNA + CDDP), $^{**}P < 0.01$ considered statistically significant compared with sc-siRNA-transfected cells (sc-siRNA). To demonstrate successful knockdown of L1-CAM, western blots of lysates from sc-siRNA- and L1-siRNA-transfected cells are included in the graphs. Membranes were reprobed with β-actin-specific antibodies to confirm equal protein loading. n.s., not significant. (**E**) Forty-eight hours after siRNA transfection, the proliferation of A498 VHL cells was measured using an MTT proliferation assay as described under Materials and Methods. $^{***}P < 0.001$ considered statistically significant compared with sc-siRNA-transfected A498 VHL cells. (**F**) Seventy-two hours after siRNA transfection, A498 VHL cells were lysed and western blot analysis were performed with L1-CAM or cyclin D1-specific antibodies. β-Actin was used to demonstrate equal protein loading.

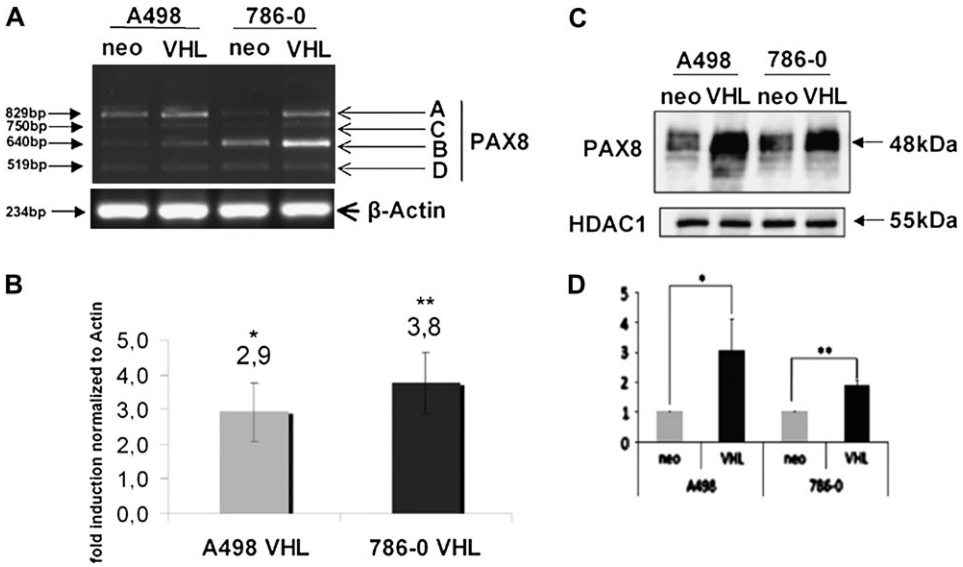

Fig. 4. Increased PAX8 levels in VHL expressing renal cancer cells. (**A**) Reverse transcription–PCR results with PAX8-specific primers in A498 neo, A498 VHL, 786 neo and 786 VHL cells. Arrows indicate the four different splice variants of PAX8 (A–D). (**B**) Real-time PCR data represent a 2.9-fold (A498 VHL) and a 3.8-fold (786-0 VHL) induction of PAX8 mRNA compared with the VHL-deficient A498 neo and 786-0 neo cells, respectively. $^{*}P < 0.05$ considered statistically significant compared with A498 neo cells. $^{**}P < 0.01$ considered statistically significant compared with 786-0 neo cells. (**C**) Western blot analysis of nuclear extracts of A498 neo, A498 VHL, 786-0 neo and 786-0 VHL cells with PAX8-specific antibodies. Membranes were reprobed with Histone deacetylase-1 antibodies to demonstrate equal sample loading. (**D**) Densitometric analysis of nuclear PAX8 protein expression shown in 3C. $^{*}P < 0.05$ considered statistically significant compared with A498 neo cells. $^{**}P < 0.01$ considered statistically significant compared with 786-0 neo cells.

the L1-CAM expression in renal cancer cells mediates also resistance against the clinically used reagents sunitinib and rapamycin. As shown in Figure 3D, the downregulation of L1-CAM in A498 VHL cells induced the cytotoxic effects of sunitinib and rapamycin, demonstrating that L1-CAM expression in renal cancer cells is involved in the resistance against clinically used therapeutic reagents.

Although the downregulation of L1-CAM did not induce apoptosis in A498 cells, we present evidence that L1-CAM is involved in the proliferation of renal cancer cells (Figure 3E). Furthermore, L1-CAM downregulation decreased the cyclin D1 expression in renal cancer cells (Figure 3F).

The transcription factor PAX8 is regulated by the VHL protein

It is known that the transcription factor PAX6 can regulate L1-CAM expression in the developing brain (23). PAX6 is not expressed in the kidney, but PAX2 and PAX8 are known to play important roles in the development of the kidney (24). To determine the mRNA expression levels of PAX8 in VHL WT and VHL-mutated renal cancer cells, we performed reverse transcription–PCR experiments. Interestingly, the splice variant PAX8A was downregulated in A498 and 786-0 neo cells (Figure 4A). In addition, in 786-0 neo cells, we observed also a strong reduction of the PAX8B splice variant. By real-time PCR, we were able to confirm that VHL WT RCC cells expressed significant higher

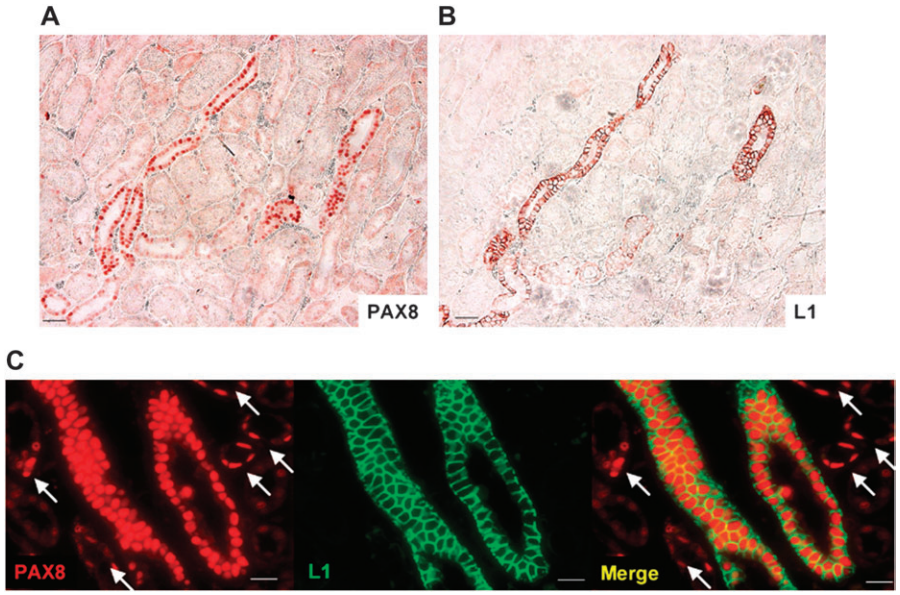

Fig. 5. L1-CAM and PAX8 are co-expressed in collecting ducts cells of normal renal tissue. Immunohistochemistry was performed on serial sections of normal renal tissue using PAX8-specific (**A**) and L1-CAM-specific (**B**) antibodies. Scale bars represent 50 μm. (**C**) Double immunofluorescense staining of PAX8 (red) and L1-CAM (green) expressing tubular cells in normal renal tissue. White arrows indicate PAX8-expressing cells, which do not express L1-CAM. Scale bars represent 20 μm.

levels of PAX8 mRNA than the VHL-deficient counterparts (Figure 4B). In addition, we confirmed with isolated nuclear proteins that VHL-deficient A498 and 786-0 cells expressed lower PAX8 protein levels compared with the VHL WT-expressing cells (Figure 4C). In Figure 4D, densitometric analysis of Figure 4C is shown.

The transcription factor PAX8 and L1-CAM colocalize in collecting duct cells of human kidney

To examine the localization of PAX8 and L1-CAM in the human kidney, we performed immunohistochemistry analysis on serial sections of normal renal tissue. Strong PAX8 expression (Figure 5A) was observed in nuclei of L1-CAM-expressing collecting duct cells (Figure 5B). These data were confirmed by immunofluorescence analysis (Figure 5C). In contrast to the immunohistochemistry data, we also found PAX8-positive tubular cells that did not express L1-CAM (Figure 5C white arrows).

PAX8 expression in renal tumor samples

The expression of PAX8 in renal cancer tissue was analyzed immunohistochemically in our TMA with 282 renal cancer samples. Representative stainings for the PAX8 expression in normal kidney and tumor samples (negative, weak and strong expression) are shown in Figure 6A. The obtained results are summarized in a diagram (Figure 6B). Only 34.7% of the analyzed renal cancer samples expressed

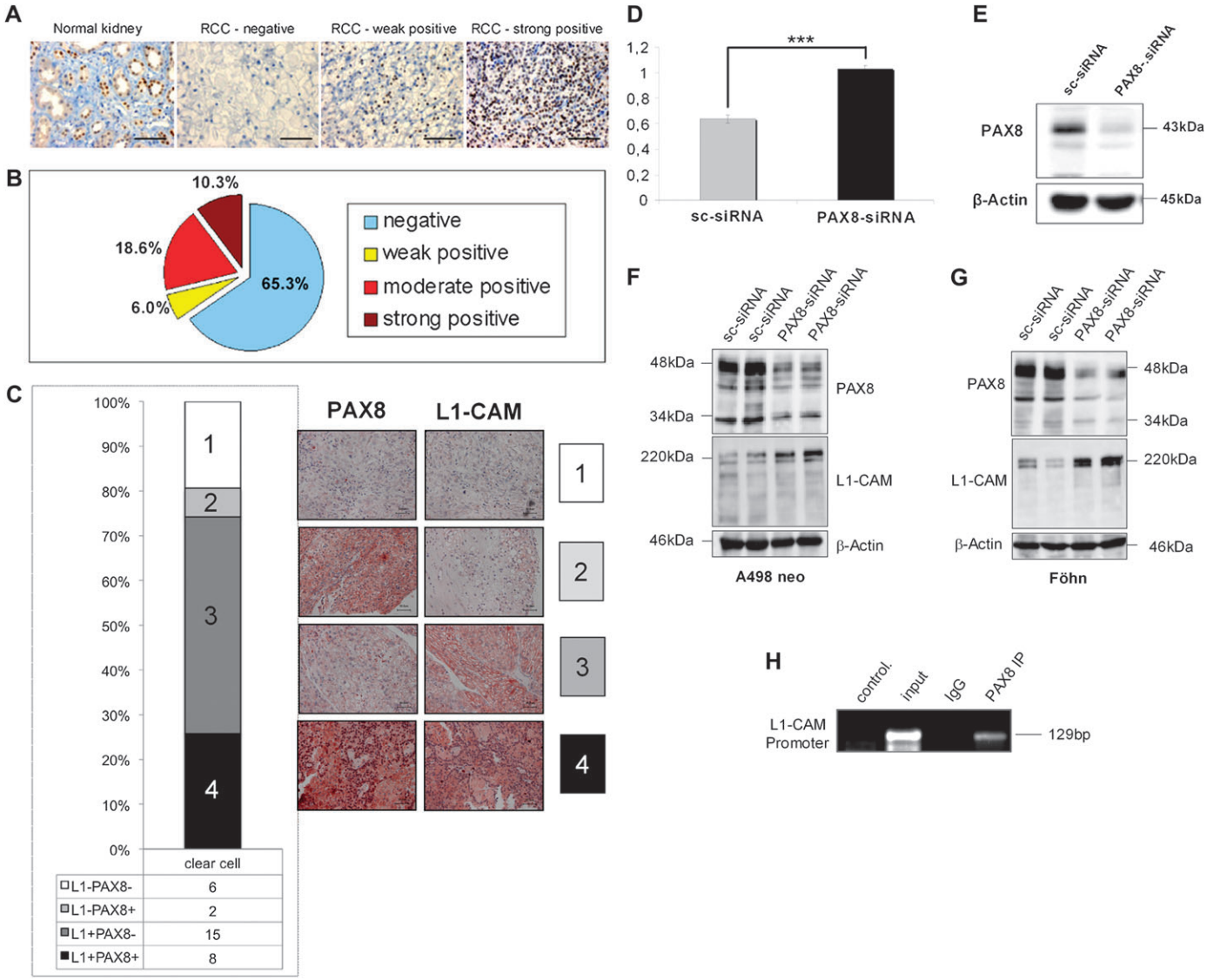

Fig. 6. Expression of PAX8 in normal renal tissue and renal cancer tissue and PAX8 knockdown increases L1-CAM expression. (**A**) Immunohistochemistry images showing the expression of PAX8 in normal kidney and a representive image of negative, weak positive and strong positive L1-CAM staining in renal cancer patients (RCC). Scale bars represent 50 μm. (**B**) Pie charts demonstrate the percentage of negative (blue), weak positive (yellow), moderate positive (red) and strong PAX8-positive (maroon) cases of RCC. (**C**) Serial sections of a TMA with 31 ccRCC patients were investigated by immunohistochemical analysis. Results were divided in four groups representing group 1: PAX8-negative and L1-CAM-negative patients, (white bar) group 2: PAX8-positive and L1-CAM-negative patients (light gray bar), group 3: PAX8-negative and L1-CAM-positive patients (gray bar) and group 4: PAX8-positive and L1-CAM-positive patients (black bar). Numbers in the bars are belonging to the respective group. Representive immunohistochemical images of each group are shown on the right side of the figure. (**D**) Forty-eight hours after sc-siRNA or PAX8-siRNA transfection, the migration of A498 neo cells were analyzed in Boyden chamber assay. $^{***}P < 0.001$ considered statistically significant compared with sc-siRNA-transfected A498 neo cells. (**E**) Seventy-two hours after the transfection with siRNA, lysates of A498 neo cells were analyzed by western blot with PAX8-specific antibodies. Equal sample loading was controlled by β-actin-specific antibodies. (**F**) A498 neo and (**G**) Föhn cells were transfected with control (sc-siRNA) or PAX8 (PAX8-siRNA). Seventy-two hours after transfection, cell lysates were investigated by western blot analysis with PAX8- or L1-CAM-specific antibodies. To confirm equal protein loading membranes were incubated with β-actin antibodies. (**H**) ChIP assay was performed in A498 VHL cells as described under Materials and Methods to demonstrate PAX8 protein binding to the L1-CAM promoter.

PAX8. The highest levels of PAX8 expression were detectable in papillary carcinomas, most of which (71.4%) were positive for PAX8. In clear cell carcinomas, the rate of PAX8 positivity was 29.1% and none of the chromophobe RCC (0/10) was positive for PAX8. In addition, we performed on serial sections of a TMA with 31 different ccRCC patients immunhistochemical analysis with L1-CAM- and PAX8-specific antibodies. Interestingly, 50% of ccRCC patients, which were negative for PAX8, showed induced L1-CAM expression (Figure 6C).

To evaluate the role of PAX8 in renal cancer cell migration, we downregulated PAX8 protein expression by specific PAX8 siRNA and performed a transwell migration assay. Interestingly, the knockdown of PAX8 increased the migration of A498 (Figure 6D). The successful knockdown of PAX8 is shown in Figure 6E. To investigate if PAX8 can regulate L1-CAM expression in RCC, we downregulated PAX8 protein expression by siRNA in A498 neo cells and Föhn cells. The downregulation of PAX8 led to a significant increase of L1-CAM protein levels in A498 (Figure 6F) and Föhn cells (Figure 6G). Similar results were obtained in 786-0 VHL and A498 VHL cells (data not shown). In addition, by ChIP analysis, we could show that PAX8 is able to bind to the L1-CAM promoter (Figure 6H).

Discussion

L1-CAM overexpression has been found in several tumors like melanoma, ovarian and colon cancer (25). In addition, the study of Meli *et al.* (26) described L1-CAM expression in renal cancer tissue. In ccRCC, conflicting data exist about the expression and role of L1-CAM in renal cancer progression. Although it has been reported that L1-CAM was expressed in 47% of ccRCC and L1-CAM expression correlated with metastasis (7), another study did not find L1-CAM expression in ccRCC specimens (8). Therefore, we reinvestigated the expression of L1-CAM in 282 RCC patients by immunohistochemical analysis. Notably, we used the same antibody for our investigations as the second study (8). In contrast to the data from Huszar *et al.* (8), we detected in 49% of ccRCC patients L1-CAM expression and more important L1-CAM expression correlated with shorter patients survival. In this context, it has been reported that L1-CAM expression correlated with poor prognosis and metastasis in ovarian cancer (27). In addition, a recent publication described L1-CAM as a novel independent prognostic factor in extrahepatic cholangiocarcinomas associated with poor patient survival (28). Furthermore, our study demonstrated that targeting L1-CAM in ccRCC may represent a new therapeutic option to overcome the resistance of renal cancer cells against therapeutic agents like cisplatin, sunitinib and rapamycin. In this line, it has been shown that L1-CAM expression confers chemoresistance in melanoma (16), pancreatic adenocarcinoma (29) and ovarian carcinoma cell lines (30). Importantly, patients with low L1-CAM expressing ovarian tumors exhibited a better response to chemotherapy and had a statistically longer progression-free survival (31), highlighting the potential therapeutic usefulness of L1-CAM as a target molecule in the treatment of ovarian cancer patients.

In normal tissue, L1-CAM expression is only found in peripheral nerve bundles and renal tubules, but increased L1-CAM levels are often found in various cancers (8). Therefore, it is crucially important to identify factors, which can regulate L1-CAM in cancer cells. Interestingly, in biopsies of VHL-mutated ccRCC patients and VHL-deficient cell lines L1-CAM was downregulated. In addition, we demonstrated that re-expression of VHL in VHL-deficient renal cancer cells increased the expression of L1-CAM in a hypoxia inducible factor-independent manner. The tumor suppressor gene VHL is inactivated in >80% of sporadic RCC (32) and re-expression of VHL in renal cancer cells prevents the tumorigenic effects in severe combined immunodeficient mice (32–35). In contrast to the tumor suppressor function of VHL in the kidney, a recent study has demonstrated that the expression of VHL WT together with low Carbonic Anhydrase IX expression was associated to a particular aggressive ccRCC phenotype (36). In addition, VHL WT together with high Vascular Endothelial Growth Factor expression was associated with tumor aggressiveness and poor survival of renal cancer patients (37). Therefore, our data suggest that VHL-induced L1-CAM expression and L1-CAM expression in ccRCC correlated with poor patients prognosis are in line with the above described studies (36,37).

In colon cancer, it has been shown that the β-catenin-T cell transcription factor transcriptional complex activates the L1-CAM gene (38). We could not identify β-catenin as a regulator of L1-CAM expression in RCC (data not shown). In contrast, we present evidence that PAX8 is involved in the regulation of L1-CAM. With CHIP analysis, we present evidence that PAX8 is able to bind to the L1-CAM promoter and the downregulation of PAX8 induced the expression of L1-CAM in VHL negative and WT renal cancer cells. Importantly, in a big fraction of ccRCC patients, PAX8 downregulation was accompanied with increased L1-CAM expression, assuming that PAX8 is a negative regulator of L1-CAM in renal cancer cells. Recently, an immunohistochemical study has characterized the expression of PAX8 in normal kidney and renal tumors (39). The expression of PAX8 in papillary RCC is basically in line with the study of Tong *et al.* (39), who also found the highest PAX8 levels in papillary RCC. However, we could not confirm the rather high rate of PAX8 positivity in our cohort of ccRCC. This might be due to methodological differences or could be explained by the existence of four PAX8 mRNA isoforms, which have been identified in human kidney cell lines (40). Interestingly, our data demonstrate that the downregulation of PAX8 increased the migration of renal cancer cells. This induction might be explained by an increase in L1-CAM expression as L1-CAM expression in normal and cancer cells is involved in enhanced cell motility (38). PAX8 and PAX2 are important developmental transcription factors in renal organogenesis (11,41,42) and are often co-expressed during development. In the developing nephric duct in mice, both PAX2 and PAX8 are required for specifying the nephric lineage (11). However, although PAX2 and PAX8 are expressed together in bladder and ovarian cancer cell lines, RNA interference against just the PAX2 gene leads to cell death (43). Therefore, a greater understanding of the coordinate interplay between different PAX proteins in development and cancer is required.

In summary, our data demonstrated that L1-CAM expression in ccRCC is associated with a poor prognosis and represents an attractive therapeutic target molecule for the treatment of ccRCC patients.

Acknowledgements

Conflict of Interest Statement: None declared.

References

1. Rini,B.I. *et al*. (2008) Renal cell carcinoma. *Curr. Opin. Oncol.*, **20**, 300–306.
2. Gupta,K. *et al*. (2008) Epidemiologic and socioeconomic burden of metastatic renal cell carcinoma (mRCC): a literature review. *Cancer Treat. Rev.*, **34**, 193–205.
3. Schrader,A.J. *et al*. (2006) Second-line strategies for metastatic renal cell carcinoma: classics and novel approaches. *J. Cancer Res. Clin. Oncol.*, **132**, 137–149.
4. Novak-Hofer,I. (2007) The L1 cell adhesion molecule as a target for radioimmunotherapy. *Cancer Biother. Radiopharm.*, **22**, 175–184.
5. Moos,M. *et al*. (1988) Neural adhesion molecule L1 as a member of the immunoglobulin superfamily with binding domains similar to fibronectin. *Nature*, **334**, 701–703.
6. Gutwein,P. *et al*. (2003) ADAM10-mediated cleavage of L1 adhesion molecule at the cell surface and in released membrane vesicles. *FASEB J.*, **17**, 292–294.
7. Allory,Y. *et al*. (2005) The L1 cell adhesion molecule is induced in renal cancer cells and correlates with metastasis in clear cell carcinomas. *Clin. Cancer Res.*, **11**, 1190–1197.
8. Huszar,M. *et al*. (2006) Expression profile analysis in multiple human tumors identifies L1 (CD171) as a molecular marker for differential diagnosis and targeted therapy. *Hum. Pathol.*, **37**, 1000–1008.
9. Raveh,S. *et al*. (2009) L1 cell adhesion molecule (L1CAM) in invasive tumors. *Cancer Lett.*, **2**, 137–145.
10. Chalepakis,G. *et al*. (1994) Characterization of Pax-6 and Hoxa-1 binding to the promoter region of the neural cell adhesion molecule L1. *DNA Cell Biol.*, **13**, 891–900.

11. Bouchard,M. *et al*. (2002) Nephric lineage specification by Pax2 and Pax8. *Genes Dev.*, **16**, 2958–2970.
12. Robson,E.J. *et al*. (2006) A PANorama of PAX genes in cancer and development. *Nat. Rev. Cancer*, **6**, 52–62.
13. Luu,V.D. *et al*. (2009) Loss of VHL and hypoxia provokes PAX2 upregulation in clear cell renal cell carcinoma. *Clin. Cancer Res.*, **15**, 3297–3304.
14. Nyhan,M.J. *et al*. (2008) Role of the VHL (von Hippel-Lindau) gene in renal cancer: a multifunctional tumour suppressor. *Biochem. Soc. Trans.*, **36**, 472–478.
15. Hergovich,A. *et al*. (2003) Regulation of microtubule stability by the von Hippel-Lindau tumour suppressor protein pVHL. *Nat. Cell Biol.*, **5**, 64–70.
16. Lee,S.B. *et al*. (2009) ADAM10 is upregulated in melanoma metastasis compared with primary melanoma. *J. Invest. Dermatol.*, **3**, 763–773.
17. Schramme,A. *et al*. (2008) Characterization of CXCL16 and ADAM10 in the normal and transplanted kidney. *Kidney Int.*, **74**, 328–338.
18. Elbashir,S.M. *et al*. (2001) Duplexes of 21-nucleotide RNAs mediate RNA interference in cultured mammalian cells. *Nature*, **411**, 494–498.
19. Fritzsche,F.R. *et al*. (2008) Claudin-1 protein expression is a prognostic marker of patient survival in renal cell carcinomas. *Clin. Cancer Res.*, **14**, 7035–7042.
20. Gutwein,P. *et al*. (2009) Downregulation of junctional adhesion molecule-A is involved in the progression of clear cell renal cell carcinoma. *Biochem. Biophys. Res. Commun.*, **380**, 387–391.
21. Mechtersheimer,S. *et al*. (2001) Ectodomain shedding of L1 adhesion molecule promotes cell migration by autocrine binding to integrins. *J. Cell Biol.*, **155**, 661–673.
22. Banks,R.E. *et al*. (2006) Genetic and epigenetic analysis of von Hippel-Lindau (VHL) gene alterations and relationship with clinical variables in sporadic renal cancer. *Cancer Res.*, **66**, 2000–2011.
23. Meech,R. *et al*. (1999) A binding site for homeodomain and Pax proteins is necessary for L1 cell adhesion molecule gene expression by Pax-6 and bone morphogenetic proteins. *Proc. Natl Acad. Sci. USA*, **96**, 2420–2425.
24. Narlis,M. *et al*. (2007) Pax2 and pax8 regulate branching morphogenesis and nephron differentiation in the developing kidney. *J. Am. Soc. Nephrol.*, **18**, 1121–1129.
25. Gavert,N. *et al*. (2008) L1-CAM in cancerous tissues. *Expert Opin. Biol. Ther.*, **8**, 1749–1757.
26. Meli,M.L. *et al*. (1999) Anti-neuroblastoma antibody chCE7 binds to an isoform of L1-CAM present in renal carcinoma cells. *Int. J. Cancer*, **83**, 401–408.
27. Zecchini,S. *et al*. (2008) The differential role of L1 in ovarian carcinoma and normal ovarian surface epithelium. *Cancer Res.*, **68**, 1110–1118.
28. Li,S. *et al*. (2009) L1 cell adhesion molecule is a novel independent poor prognostic factor of extrahepatic cholangiocarcinoma. *Clin. Cancer Res.*, **15**, 7345–7351.
29. Sebens,M.S. *et al*. (2007) Drug-induced expression of the cellular adhesion molecule L1CAM confers anti-apoptotic protection and chemoresistance in pancreatic ductal adenocarcinoma cells. *Oncogene*, **26**, 2759–2768.
30. Stoeck,A. *et al*. (2007) L1-CAM in a membrane-bound or soluble form augments protection from apoptosis in ovarian carcinoma cells. *Gynecol. Oncol.*, **104**, 461–469.
31. Daponte,A. *et al*. (2008) L1 (CAM) (CD171) in ovarian serous neoplasms. *Eur. J. Gynaecol. Oncol.*, **29**, 26–30.
32. Kaelin,W.G. Jr. (2008) The von Hippel-Lindau tumour suppressor protein: O2 sensing and cancer. *Nat. Rev. Cancer*, **8**, 865–873.
33. Gnarra,J.R. *et al*. (1996) Molecular cloning of the von Hippel-Lindau tumor suppressor gene and its role in renal carcinoma. *Biochim. Biophys. Acta*, **1242**, 201–210.
34. Iliopoulos,O. *et al*. (1995) Tumour suppression by the human von Hippel-Lindau gene product. *Nat. Med.*, **1**, 822–826.
35. Schoenfeld,A. *et al*. (1998) A second major native von Hippel-Lindau gene product, initiated from an internal translation start site, functions as a tumor suppressor. *Proc. Natl Acad. Sci. USA*, **95**, 8817–8822.
36. Patard,J.J. *et al*. (2008) Low CAIX expression and absence of VHL gene mutation are associated with tumor aggressiveness and poor survival of clear cell renal cell carcinoma. *Int. J. Cancer*, **123**, 395–400.
37. Patard,J.J. *et al*. (2009) Absence of VHL gene alteration and high VEGF expression are associated with tumour aggressiveness and poor survival of renal-cell carcinoma. *Br. J. Cancer*, **101**, 1417–1424.
38. Gavert,N. *et al*. (2005) L1, a novel target of beta-catenin signaling, transforms cells and is expressed at the invasive front of colon cancers. *J. Cell Biol.*, **168**, 633–642.
39. Tong,G.X. *et al*. (2009) Expression of PAX8 in normal and neoplastic renal tissues: an immunohistochemical study. *Mod. Pathol.*, **22**, 1218–1227.
40. Kozmik,Z. *et al*. (1993) Alternative splicing of Pax-8 gene transcripts is developmentally regulated and generates isoforms with different transactivation properties. *Mol. Cell. Biol.*, **13**, 6024–6035.
41. Dressler,G.R. (2006) The cellular basis of kidney development. *Annu. Rev. Cell Dev. Biol.*, **22**, 509–529.
42. Eccles,M.R. *et al*. (2002) PAX genes in development and disease: the role of PAX2 in urogenital tract development. *Int. J. Dev. Biol.*, **46**, 535–544.
43. Muratovska,A. *et al*. (2003) Paired-Box genes are frequently expressed in cancer and often required for cancer cell survival. *Oncogene*, **22**, 7989–7997.

Received July 9, 2010; revised October 19, 2010; accepted November 14, 2010